

High Performance Infrared Focal Plane Arrays

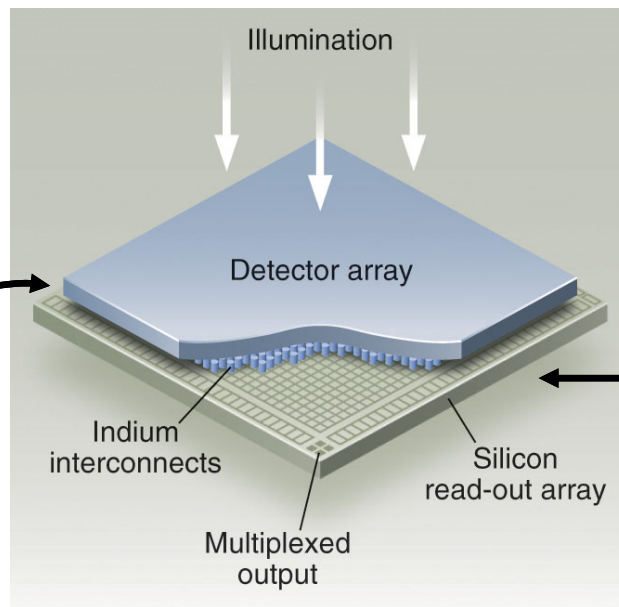
Good Attributes and Bad Attributes

Prepared by Majid Zandian, Bo Shojaei, and James Beletic

**Presented by
James W. Beletic, Ph.D.
Chief Scientific Officer
Teledyne Digital Imaging**

**Presented at
Image Sensors for Precision Astronomy
ISPA 2024
Kavli Institute for Particle Astrophysics and Cosmology (KIPAC) at SLAC
12 March 2024**

Hybrid CMOS Imaging Sensor



Detector

- Wavelength (λ)
- Quantum Efficiency
- Dark current & Noise
- Radiation environment
- Persistence

The functionality ("the brains") of a CMOS-based sensor is provided by the readout circuit

Readout Integrated Circuit (ROIC)

Input signal

- Flux – object and background

Operating Mode

- Integration time
- Frame readout time
- Shutter (rolling, snapshot)
- Multiple storage cells per pixel
- Windows
- Reset (pixel, line, global)
- Event driven

Interface

- Input (analog, digital)
- Output (analog, digital)
- # of readout ports

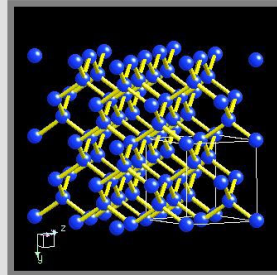
Environment

- Temperature
- Radiation

Other Requirements

- Linearity
- Anti-blooming

Periodic Table



1 H Hydrogen 1.0																	2 He Helium 4.0
3 Li Lithium 6.9	4 Be Beryllium 9.0											5 B Boron 10.8	6 C Carbon 12.0	7 N Nitrogen 14.0	8 O Oxygen 16.0	9 F Fluorine 19.0	10 Ne Neon 20.2
11 Na Sodium 23.0	12 Mg Magnesium 9.0											13 Al Aluminum 27.0	14 Si Silicon 28.1	15 P Phosphorus 31.0	16 S Sulfur 32.1	17 Cl Chlorine 35.5	18 Ar Argon 36.0
19 K Potassium 39.1	20 Ca Calcium 40.2	21 Sc Scandium 45.0	22 Ti Titanium 47.9	23 V Vanadium 50.9	24 Cr Chromium 52.0	25 Mn Manganese 54.9	26 Fe Iron 55.9	27 Co Cobalt 58.9	28 Ni Nickel 58.7	29 Cu Copper 63.5	30 Zn Zinc 65.4	31 Ga Gallium 69.7	32 Ge Germanium 72.6	33 As Arsenic 74.9	34 Se Selenium 79.0	35 Br Bromine 79.9	36 Kr Krypton 83.8
37 Rb Rubidium 85.5	38 Sr Strontium 87.6	39 Y Yttrium 88.9	40 Zr Zirconium 91.2	41 Nb Niobium 92.9	42 Mo Molybdenum 95.9	43 Tc Technetium 99	44 Ru Ruthenium 101.0	45 Rh Rhodium 102.9	46 Pd Palladium 106.4	47 Ag Silver 107.9	48 Cd Cadmium 112.4	49 In Indium 114.8	50 Sn Tin 118.7	51 Sb Antimony 121.8	52 Te Tellurium 127.6	53 I Iodine 126.9	54 Xe Xenon 131.3
55 Cs Caesium 132.9	56 Ba Barium 137.4	57-71 Lanthanides	72 Hf Hafnium 178.5	73 Ta Tantalum 181.0	74 W Tungsten 183.9	75 Re Rhenium 186.2	76 Os Osmium 190.2	77 Ir Iridium 192.2	78 Pt Platinum 195.1	79 Au Gold 197.0	80 Hg Mercury 200.6	81 Tl Thallium 204.4	82 Pb Lead 207.2	83 Bi Bismuth 209.0	84 Po Polonium 210.0	85 At Astatine 210.0	86 Rn Radon 222.0
87 Fr Francium 223.0	88 Ra Radium 226.0	89-103 Actinides	104 Rf Rutherfordium 261	105 Db Dubnium 262	106 Sg Seaborgium 263	107 Bh Bohrium 262	108 Hs Hassium 265	109 Mt Meitnerium 266	110 Uun Ununilium 272								

II III IV V VI

Detector Families

Si - IV semiconductor
HgCdTe - II-VI semiconductor
InGaAs & InSb - III-V semiconductors

- Types of Elements Key:
- Alkali metal
 - Alkaline earth metal
 - Transition metal
 - Lanthanides
 - Actinides
 - Poor metal
 - Semi-metal
 - Non-metal
 - Noble gases

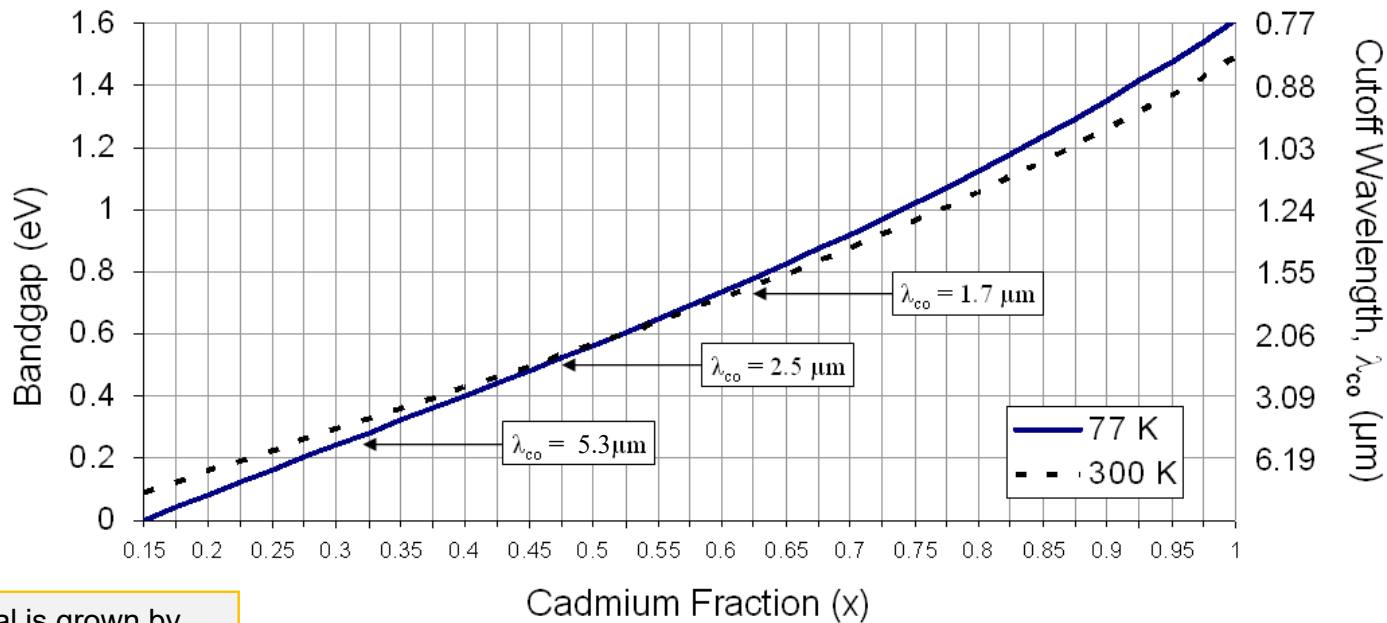
57 La Lanthanum 138.9	58 Ce Cerium 140.1	59 Pr Praseodymium 140.9	60 Nd Neodymium 144.2	61 Pm Promethium 147.0	62 Sm Samarium 150.4	63 Eu Europium 152.0	64 Gd Gadolinium 157.3	65 Tb Terbium 158.9	66 Dy Dysprosium 162.5	67 Ho Holmium 164.9	68 Er Erbium 167.3	69 Tm Thulium 168.9	70 Yb Ytterbium 173.0	71 Lu Lutetium 175.0
89 Ac Actinium 132.9	90 Th Thorium 232.0	91 Pa Protactinium 231.0	92 U Uranium 238.0	93 Np Neptunium 237.0	94 Pu Plutonium 242.0	95 Am Americium 243.0	96 Cm Curium 247.0	97 Bk Berkelium 247.0	98 Cf Californium 251.0	99 Es Einsteinium 254.0	100 Fm Fermium 253.0	101 Md Mendelevium 258.0	102 No Nobelium 254.0	103 Lr Lawrencium 260.0

Tunable Wavelength: Unique property of HgCdTe

$\text{Hg}_{1-x}\text{Cd}_x\text{Te}$ Modify ratio of Mercury and Cadmium to “tune” the bandgap energy

	II	III	IV	V	VI
	5 B Boron 10.8	6 C Carbon 12.0	7 N Nitrogen 14.0	8 O Oxygen 16.0	
	13 Al Aluminum 26.9	14 Si Silicon 28.1	15 P Phosphorus 30.9	16 S Sulfur 32.1	
	30 Zn Zinc 65.4	31 Ga Gallium 69.7	32 Ge Germanium 72.6	33 As Arsenic 74.9	34 Se Selenium 78.6
	48 Cd Cadmium 112.4	49 In Indium 114.8	50 Sn Tin 118.7	51 Sb Antimony 121.8	52 Te Tellurium 127.6
	80 Hg Mercury 200.6	81 Tl Thallium 204.4	82 Pb Lead 207.2	83 Bi Bismuth 209.0	84 Po Polonium 210.0

Bandgap and Cutoff Wavelength as function of Cadmium Fraction (x)

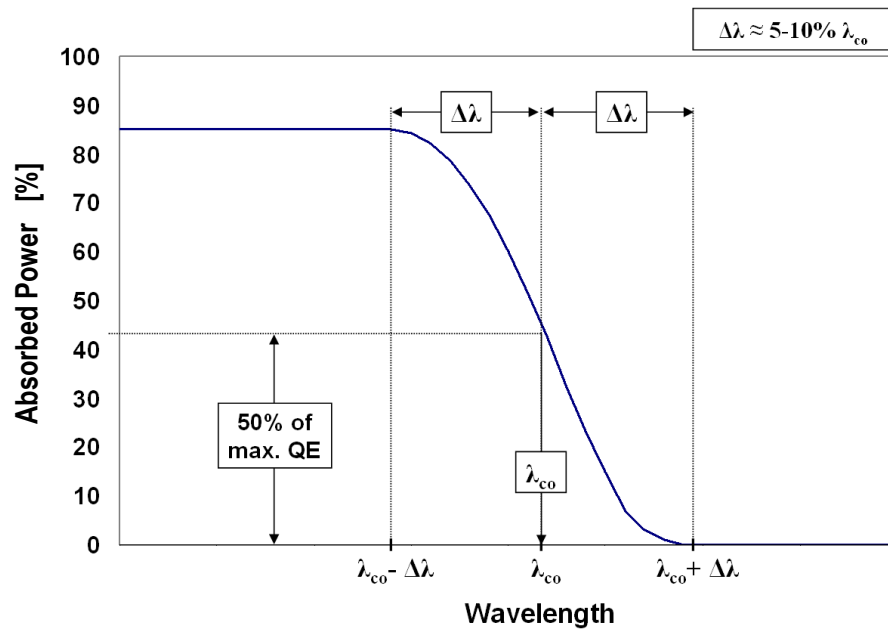


HgCdTe crystal is grown by Molecular Beam Epitaxy (MBE) on CdZnTe Substrates

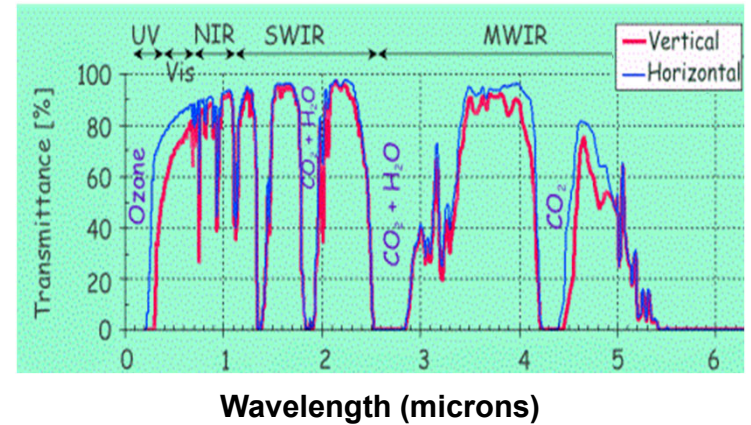
$$E_g = -0.302 + 1.93x - 0.81x^2 + 0.832x^3 + 5.35 \times 10^{-4} T(1 - 2x)$$

G. L. Hansen, J. L. Schmidt, T. N. Casselman, J. Appl. Phys. 53(10), 1982, p. 7099

HgCdTe Cutoff Wavelength



Atmospheric Transmission

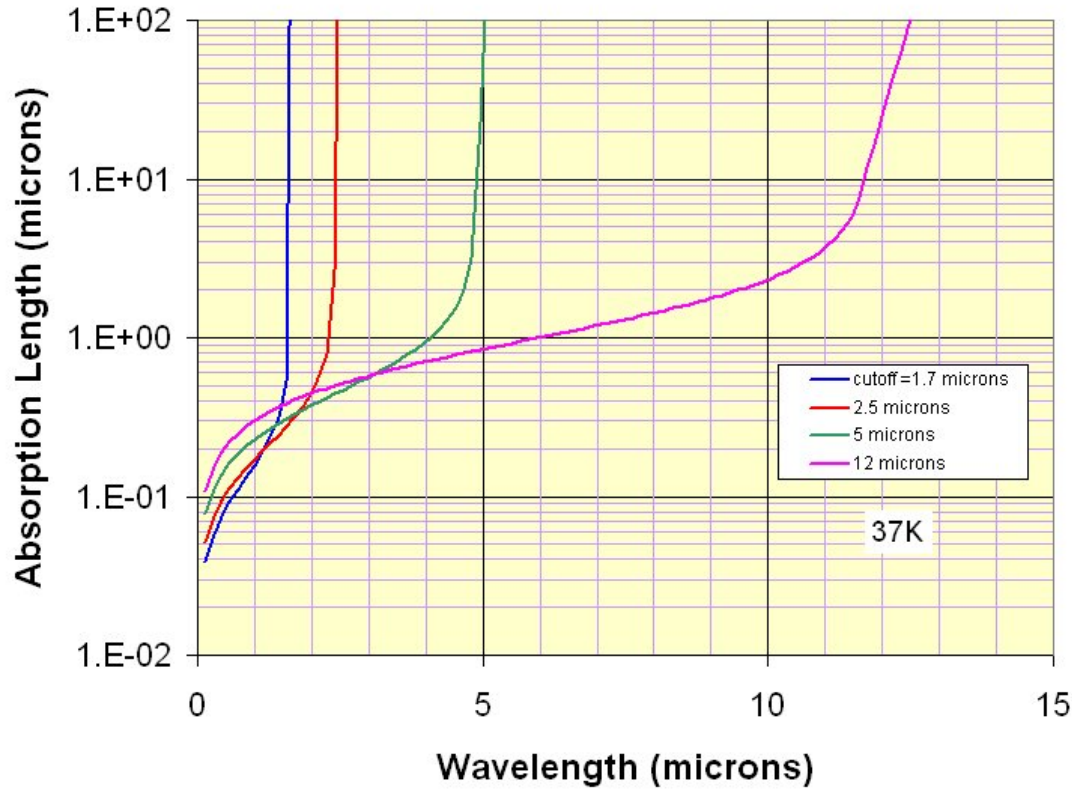


The cutoff wavelength, λ_{co} , is defined as the wavelength at which the absorbed optical power falls to half of the maximum value.

Ground-based astronomy cutoff wavelengths based on atmospheric windows

Near infrared (NIR)	1.75 μm	J,H
Short-wave infrared (SWIR)	2.5 μm	J,H,K
Mid-wave infrared (MWIR)	5.3 μm	J,H,K,L,M

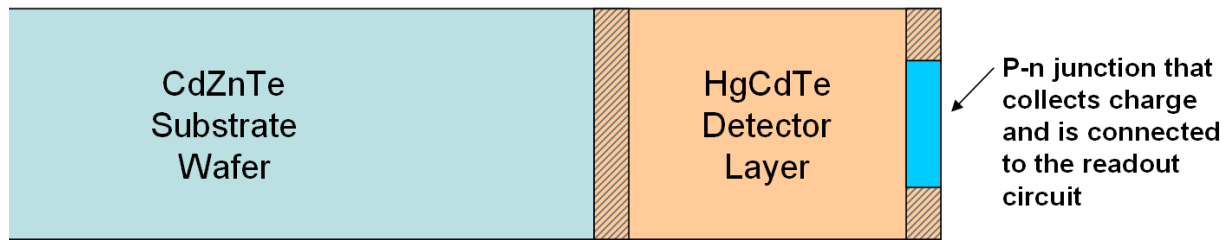
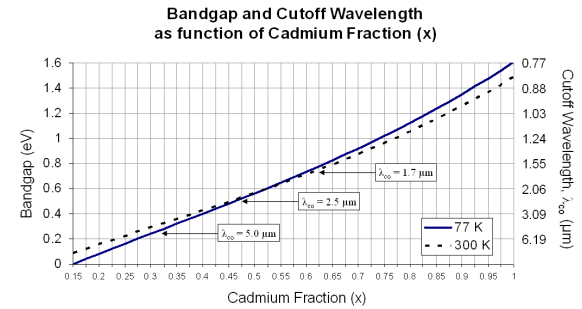
Absorption Depth of HgCdTe



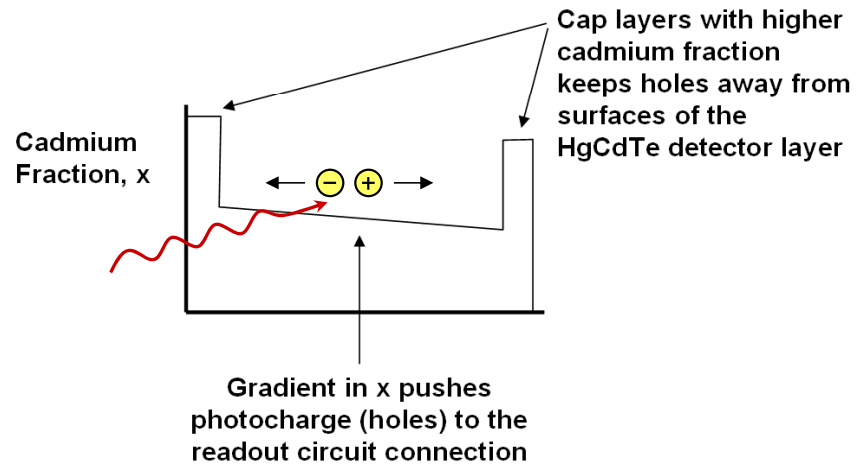
Rule of Thumb
Thickness of HgCdTe layer needs to be about equal to the cutoff wavelength (wavelength in a vacuum)

- HgCdTe is a direct bandgap material.
- HgCdTe is extremely efficient at converting electromagnetic energy into free electrons.
- The electromagnetic energy can come from photons or electrons accelerated through the material.

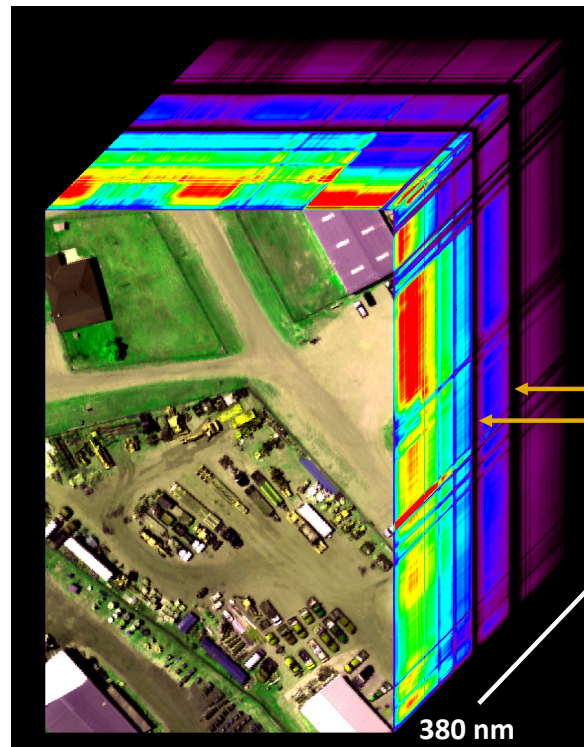
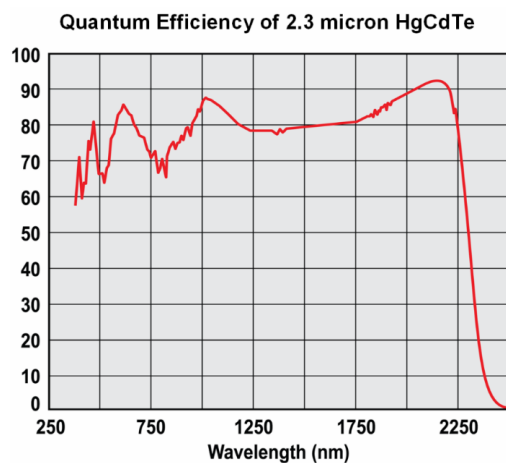
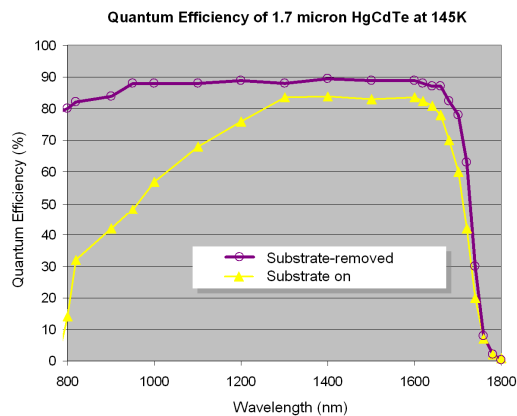
Growth Structure of p-on-n HgCdTe arrays



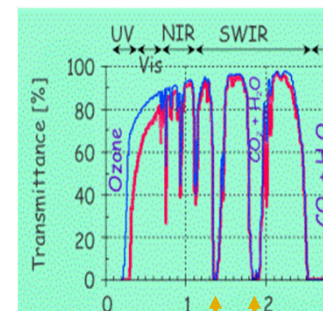
	II	III	IV	V	VI
		B Boron 10.8	C Carbon 12.0	N Nitrogen 14.0	O Oxygen 16.0
		Al Aluminum 27.0	Si Silicon 28.1	P Phosphorus 31.0	S Sulfur 32.1
30	Zn Zinc 65.4	Ga Gallium 69.7	Ge Germanium 72.6	As Arsenic 74.9	Se Selenium 79.0
48	Cd Cadmium 112.4	In Indium 114.8	Sn Tin 118.7	Sb Antimony 121.8	Te Tellurium 127.6
80	Hg Mercury 200.6	Tl Thallium 204.4	Pb Lead 207.2	Bi Bismuth 209.0	Po Polonium 210.0



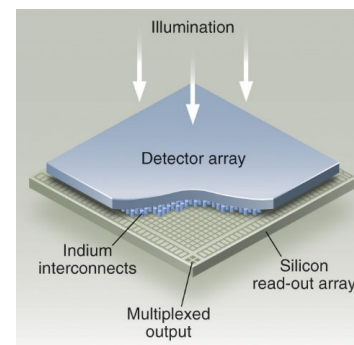
Substrate Removed HgCdTe Provides Simultaneous UV-Vis-IR Light Detection



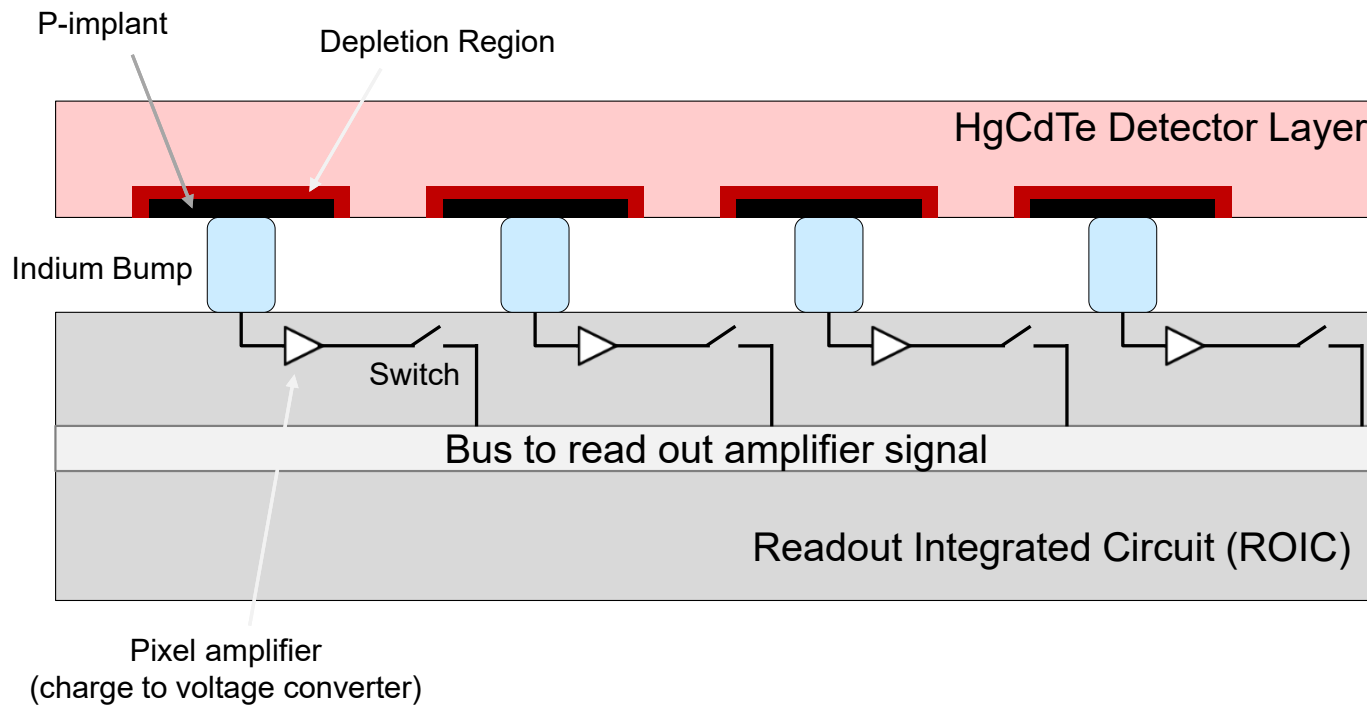
JPL AVIRIS-NG
Imaging Spectrometer



Atmospheric water vapor absorption bands at 1400 and 1900 nm

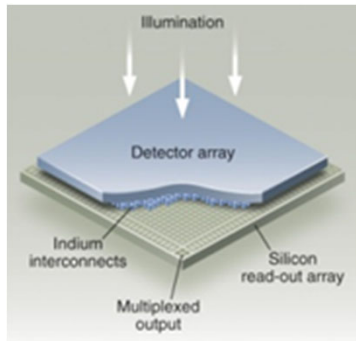


Hybrid Imager Cross Section



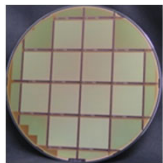
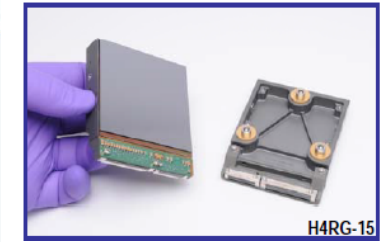
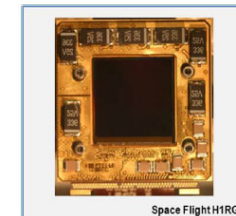
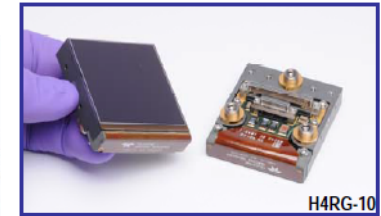
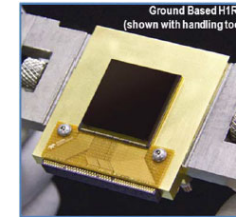


HxRG Family of Hybrid Imaging Sensors

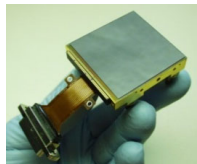


H: HAWAII: **H**gCdTe **A**stronomical **W**ide **A**rea **I**nfrared **I**mager
x: Number of 1024 (or 1K) pixel blocks in x and y-dimensions
R: **R**eference pixels
G: **G**uide window capability

- Substrate-removed HgCdTe for simultaneous visible & IR
- Hybrid Visible Silicon Imager; Si-PIN (HyViSI)



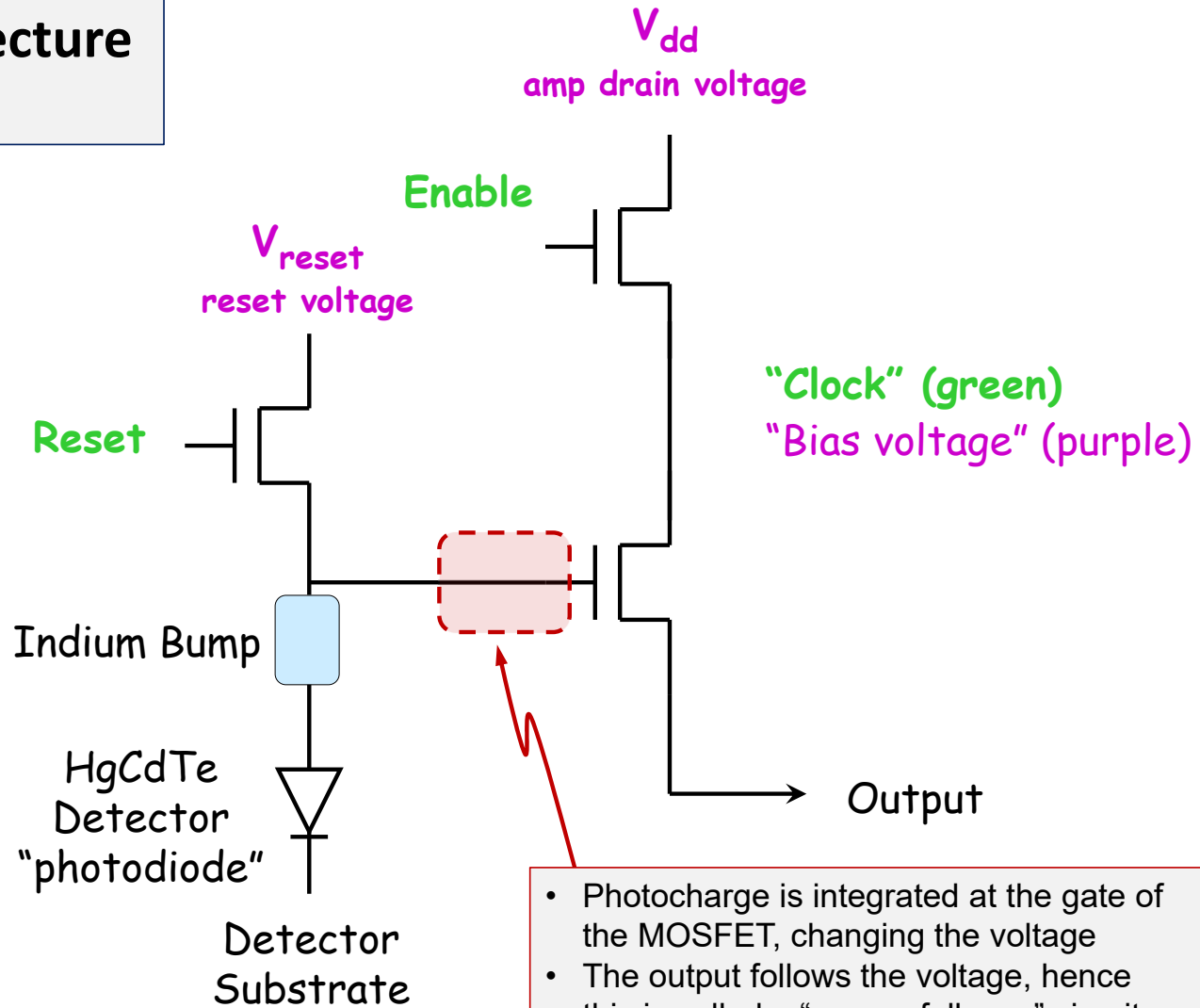
H2RG



Name	Format (# of pixels)	Pixel Pitch (microns)	# of Outputs	NASA TRL	Institutions, Observatories, & Programs using HxRG Arrays Missions / Instruments discussed at ISPA 2024 shown in bold blue
H1RG	1024 x 1024	18	1, 2, 16	9	Wide Field Survey Explorer (WISE) Orbiting Carbon Observatory (OCO), OSIRIS-REx, Ground-based Astronomy, HST (H1R) , ESA MAJIS, ESA ARIEL
H2RG	2048 x 2048	18	1, 4, 32	9	Calar Alto, Caltech, CFHT, ESO, ESA (Euclid), ESTEC, IRTF, ISRO, IUCAA, JHU-APL, Keck, Kyoto Sangyo Univ., LBNL, LMU, MIT, MPIA, MPS, NASA (James Webb Space Telescope (JWST), Joint Dark Energy Mission (JDEM)), OCIW, PSU, RIT, SALT, SAO, Subaru, TAT, U. Arizona, UCLA, UC Berkeley, U. Hawaii, U. Rochester, U. Tokyo, U. Toronto, U. Wisconsin, Dominion Astrophysics Observatory, SPHEREx.
H4RG-10	4096 x 4096	10	1, 4, 16, 32, 64	8	Joint Miliarcsecond Pathfinder Survey (JMAPS), Roman Space Telescope
H4RG-15	4096 x 4096	15	1, 4, 16, 32, 64	9	U. Hawai'i, Gemini Observatory, Subaru, CFHT, ESO (MOONS) , PIANO (Aerospace instrument on the International Space Station)

HxRG Pixel Architecture

"Source follower"

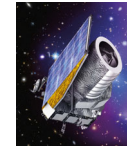


Good Attributes of HxRG arrays

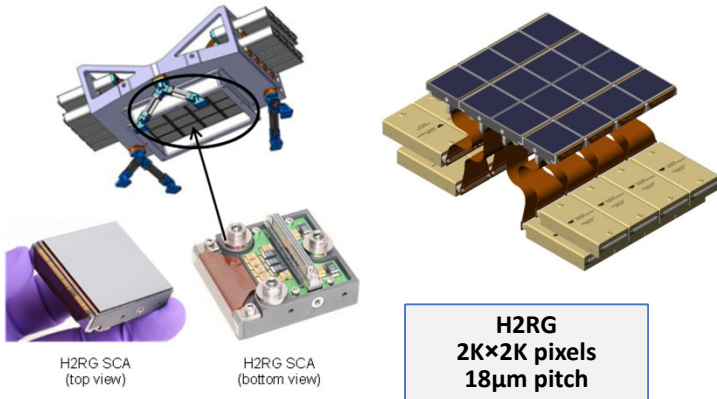
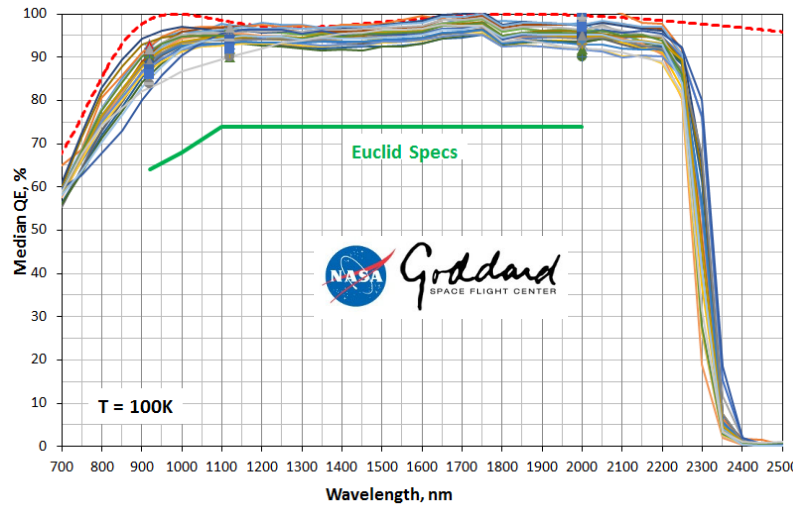
- **High Quantum Efficiency**
- **Low Dark Current**
- **Low Readout Noise**
- **Very low power**
- **Many pixels:**
 - 1, 4, or 16 million pixels per array (H1RG / H2RG / H4RG)
 - Mosaics up to 300 million pixels (Roman Space Telescope)



Teledyne Visible and IR Detectors for Euclid



- Euclid is the ESA's flagship astronomy mission.
- Launched on July 1, 2023.
- Euclid has a 1.2-m diameter large field of view telescope with visible and infrared arrays produced by Teledyne:
 - 600 million visible pixels
 - 36 4K×4K (16 Mpix) CCDs
 - 64 million infrared pixels
 - 16 H2RG (4 Mpix) SWIR arrays
 - 16 SIDECAR ASIC modules
- Largest IR focal plane array launched into space
- **24 flight candidate H2RGs delivered to NASA**
- **NASA tested and delivered 20 flight grade H2RG arrays to ESA, all of which greatly exceed requirements**



Quantum Efficiency of 24 flight candidate H2RGs

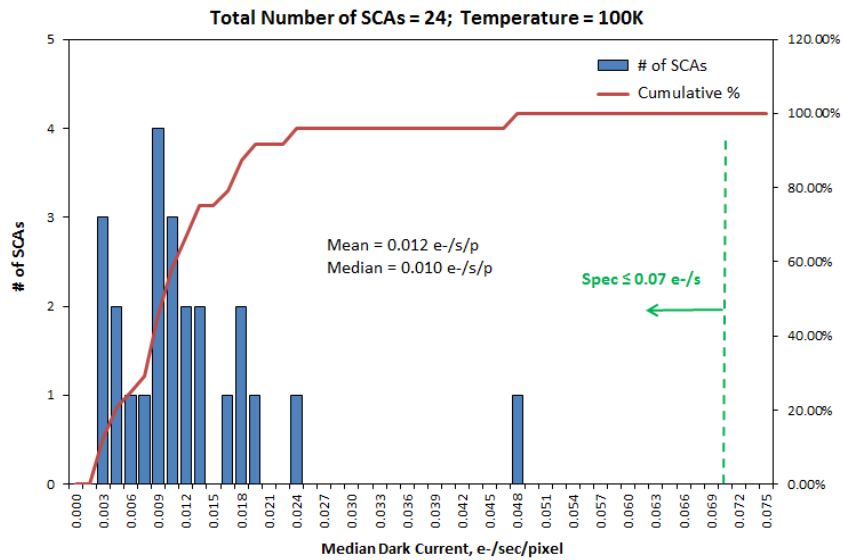
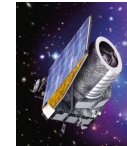
Measured by Goddard SFC Detector Characterization Laboratory

The "Hidden Galaxy" (IC 342)

- One hour observation
- 8800 x 8800 pixels
- Four bands of VIS and NISP data observed
- Three bands displayed:
 - 0.7 µm → blue
 - 1.1 µm → green
 - 1.7 µm → red



H2RG IR Detectors for Euclid

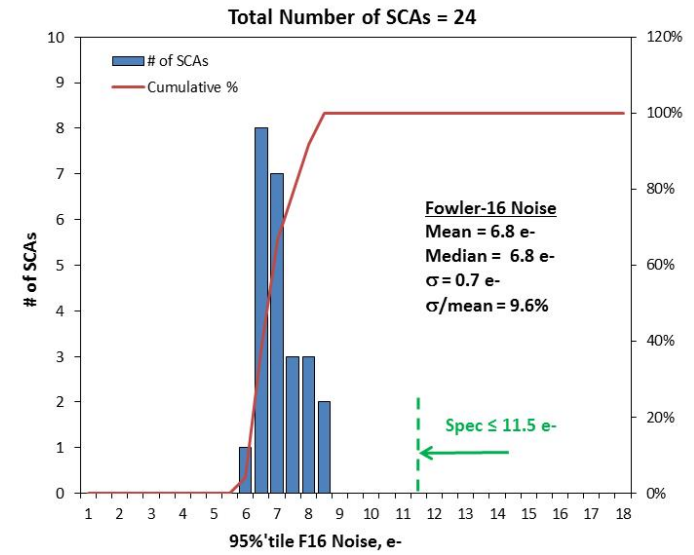


Dark Current at 100K

Median = 0.012 e-/pix/sec

More than 5X better than specification (0.07 e-/pix/sec)

2.3 μ m cutoff wavelength



Readout Noise

Median = 6.8 e-

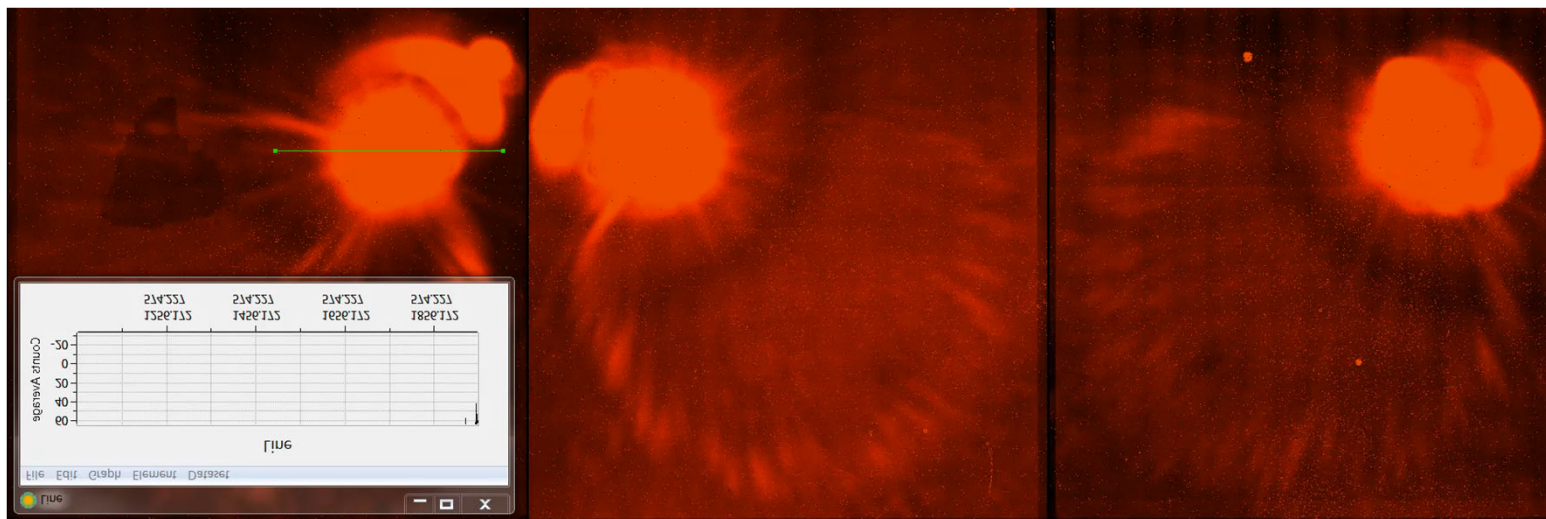
40% better than specification (11.5 e-)

Imperfections of HxRG arrays

- 1. Persistence** Memory (afterglow) of previous image
Bright calibration frames can cause big problems
- 2. Inter-Pixel Capacitance** Electrical crosstalk
- 3. Brighter-fatter effect** Intensity-dependent Point Spread Function (PSF)
- 4. Non-linearity** For highest precision, must correct each pixel
- 5. Charge diffusion** Pixel PSF is not ideal top-hat function
- 6. Cross Hatching** Intra-pixel QE variation
- 7. Bad pixels / cosmetics** Can dither to “fill in” bad pixels
- 8. Epoxy voids** Slight responsivity difference corrected by flat fielding

HxRG Imperfections: #1 Persistence

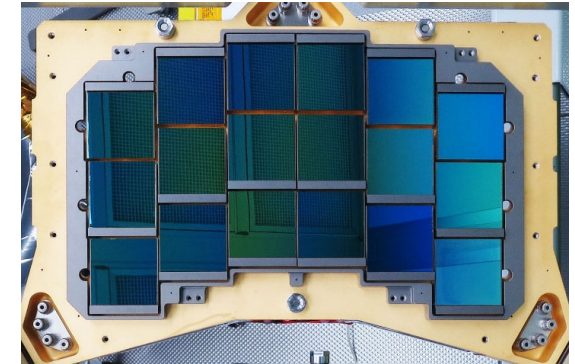
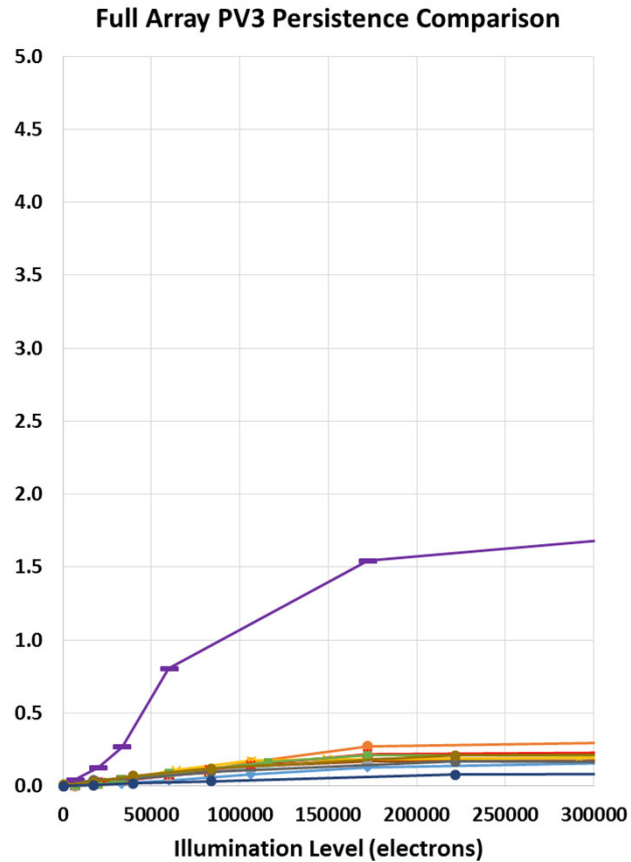
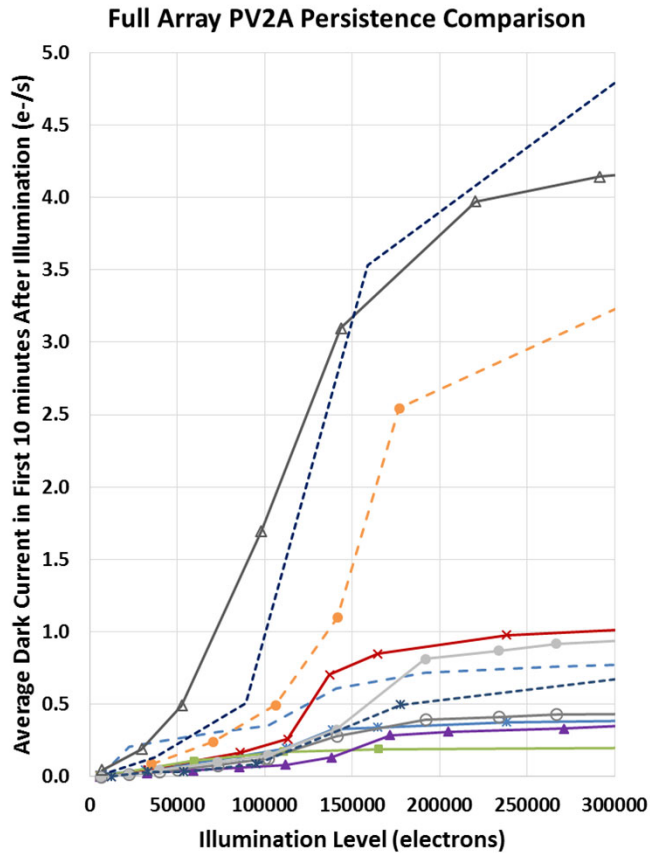
- European Southern Observatory CRIRES+ instrument has 3 MWIR H2RG arrays
- To demonstrate persistence:
 - CRIRES+ detectors exposed to an LED flash for a few milliseconds.
 - LED switched off and the detectors are read out with reset-read every 30 sec for a few minutes



Courtesy of Derek Ives, European Southern Observatory

HxRG Imperfections: #1 Persistence

The Roman Space Telescope (RST) worked closely with Teledyne during 2014-2018 to develop a new passivation process (PV3) that has shown near zero persistence.



- The low persistence process works
 - But has low yield, higher cost
- PV3 is not Teledyne's baseline process
 - Customers can request PV3 (the RST process) for custom production

HxRG Imperfections: #2 Inter-pixel capacitance (IPC)

First identified in a 2005 paper

CONVERSION GAIN AND INTERPIXEL CAPACITANCE OF CMOS HYBRID FOCAL PLANE ARRAYS

Nodal capacitance measurement by a capacitance comparison technique

G. Finger¹, J. Beletic², R. Dorn¹, M. Meyer¹, L. Mehrgan¹, A.F.M. Moorwood¹, J. Stegmeier¹
¹European Southern Observatory, ²Rockwell Scientific Company

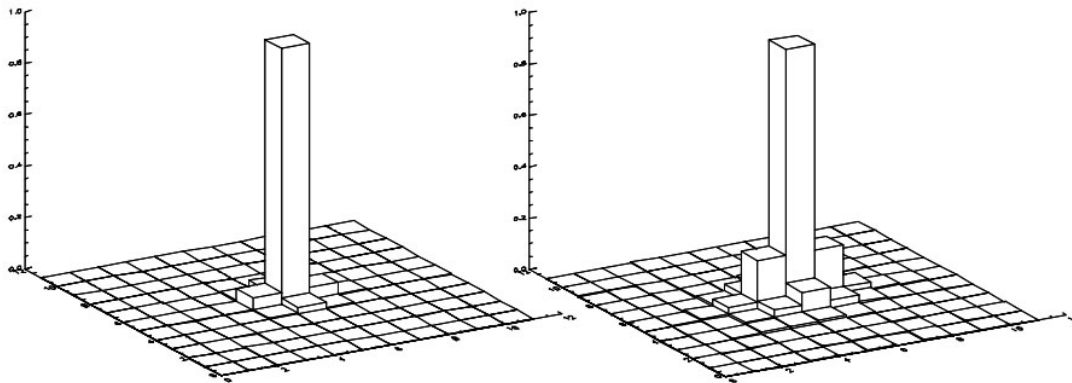
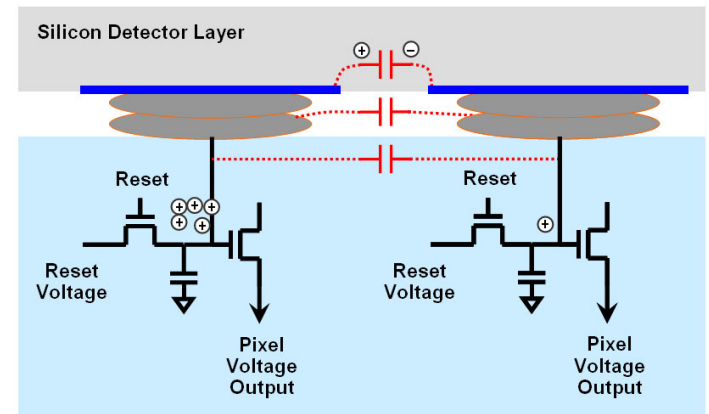


Figure 10. Autocorrelation of CMOS Hawaii-2RG hybrid arrays. Left: $\lambda_c=2.5 \mu\text{m}$ HgCdTe array, $\phi=1.23$. Right: Si-PIN HyViSI array, $\phi=2.03$.

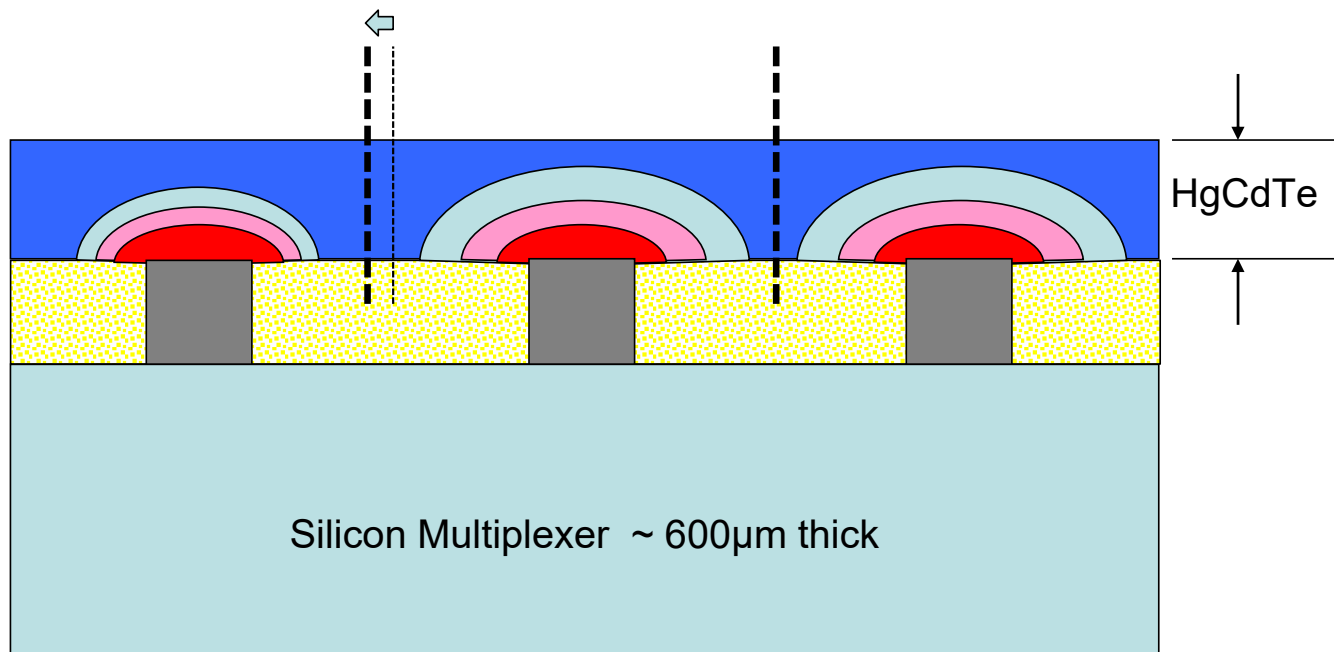


IPC can be de-convolved

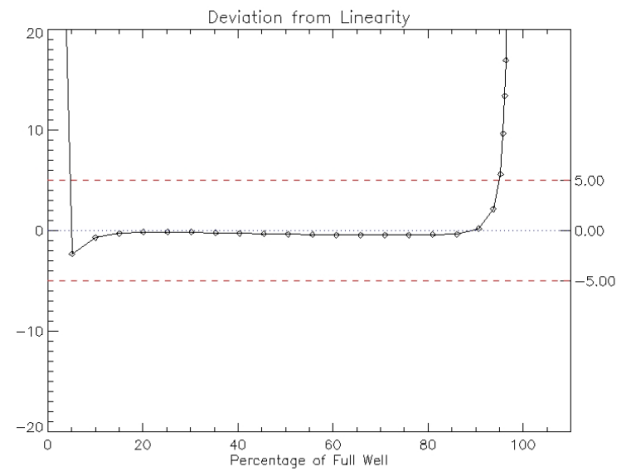
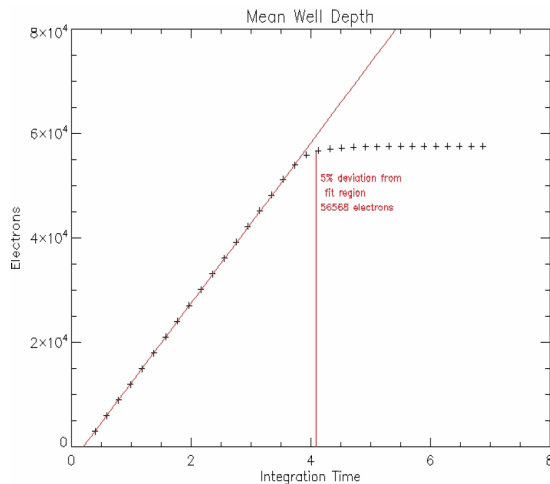
HxRG Imperfections: #3 “Brighter-fatter” effect

Figure courtesy of Roger Smith, Caltech

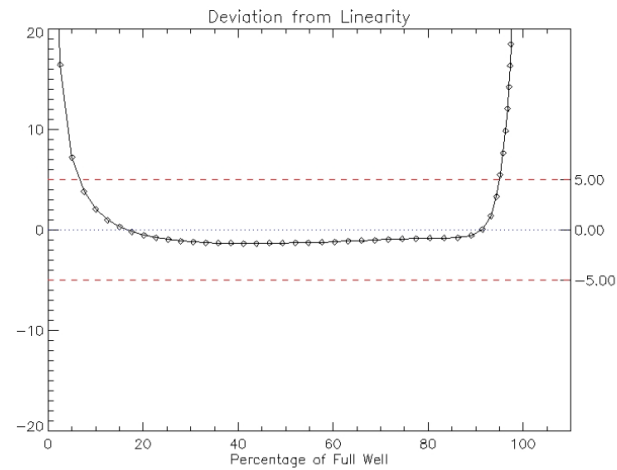
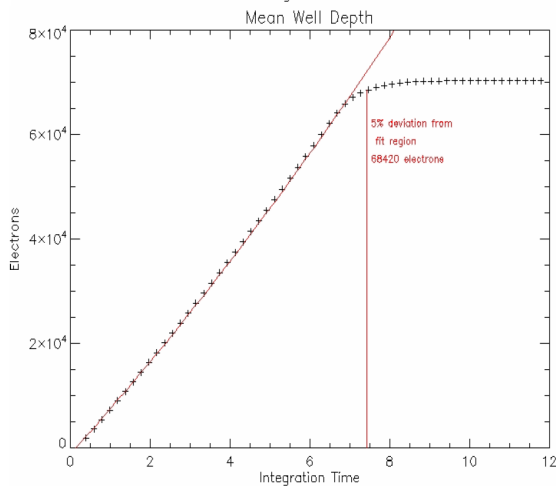
Pixel grows as charge accumulates so the point spread function (PSF) may be flux dependent



HxRG Imperfections: #4 Non-linearity (of source follower pixel)



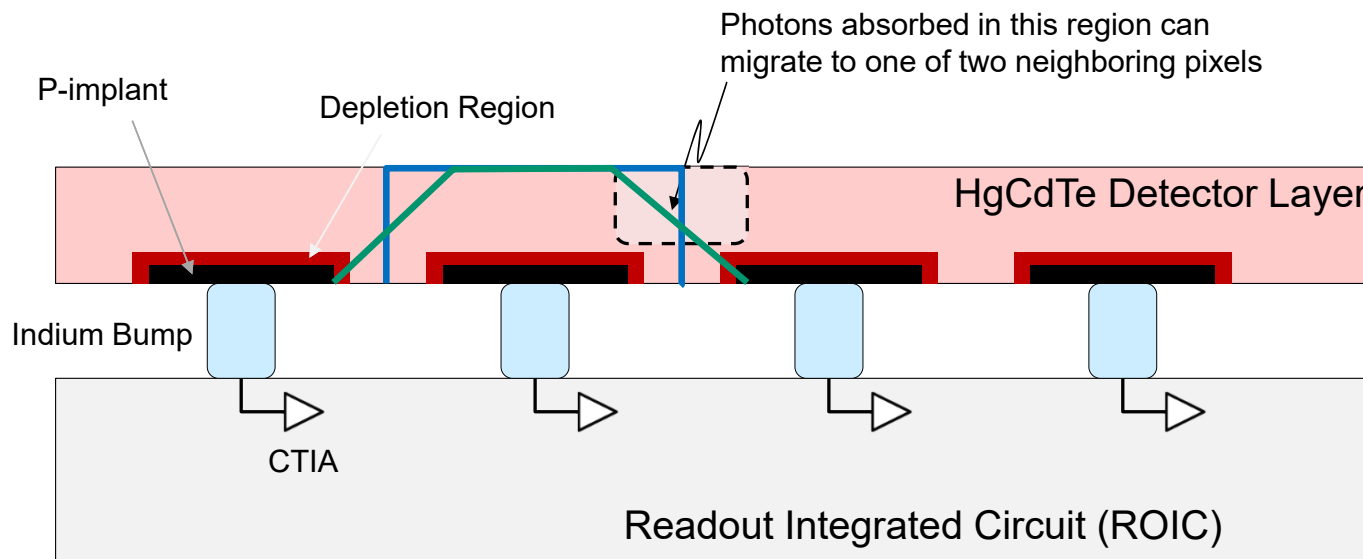
Full well defined as 5% variation from linear response



- Can correct for non-linearity at the pixel level.
- “Computationally intensive but required”

Examples from H1RG MWIR testing

HxRG Imperfections: #5 Charge Diffusion



Ideal pixel response ("top-hat" function)

Charge diffusion function

HxRG Imperfections: #6 Cross Hatching

- Cross hatching is an intra-pixel effect and very hard (impossible?) to correct with post-detection image processing.
- Need to find and fix the root cause.

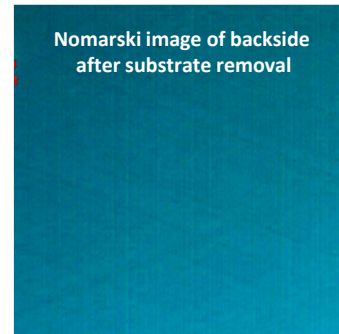
- Cross hatching observed in QE map is believed to be correlated with detector material morphology
- We believe we understand the physical mechanisms governing the morphology and can control it to an impactful degree
- Process developments are underway, full focal plane array testing has not yet started

Demonstration of detector material morphology control (as-grown surface)

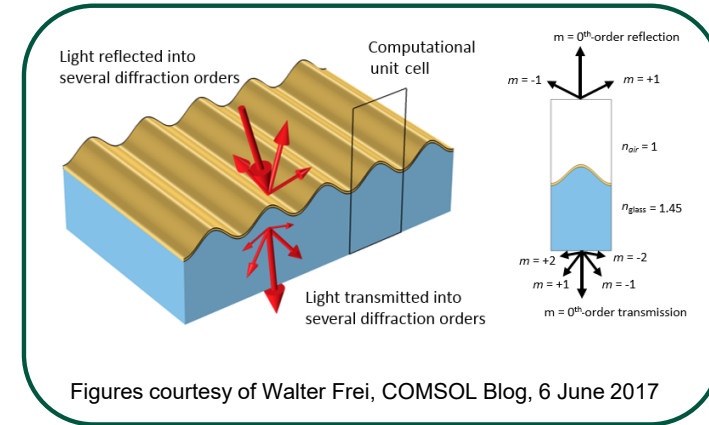


- Optical microscopy images are presented in false color and with increased saturation to help the viewer distinguish surface cross hatch.

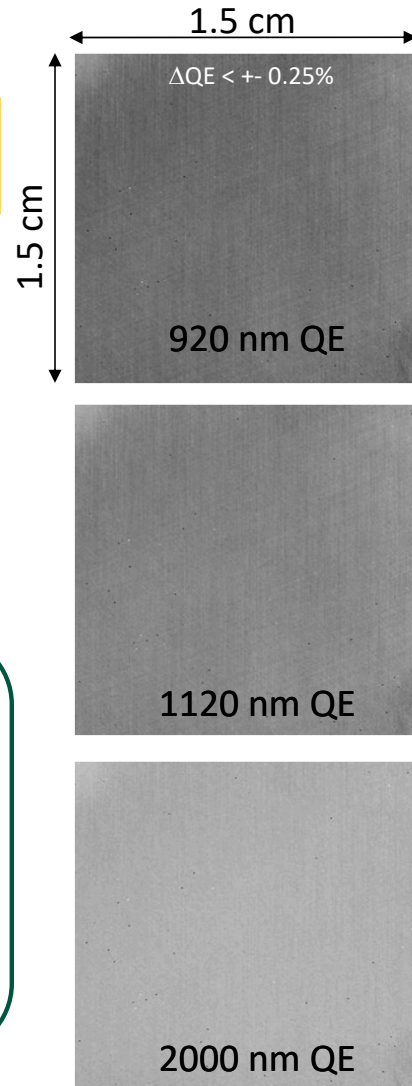
- Light from one pixel is diffracted to neighboring pixels
 - 0.2% to 0.5% QE variation of flat field illumination
 - Less QE variation for longer wavelengths



Cross hatching features are smaller than pixel dimension

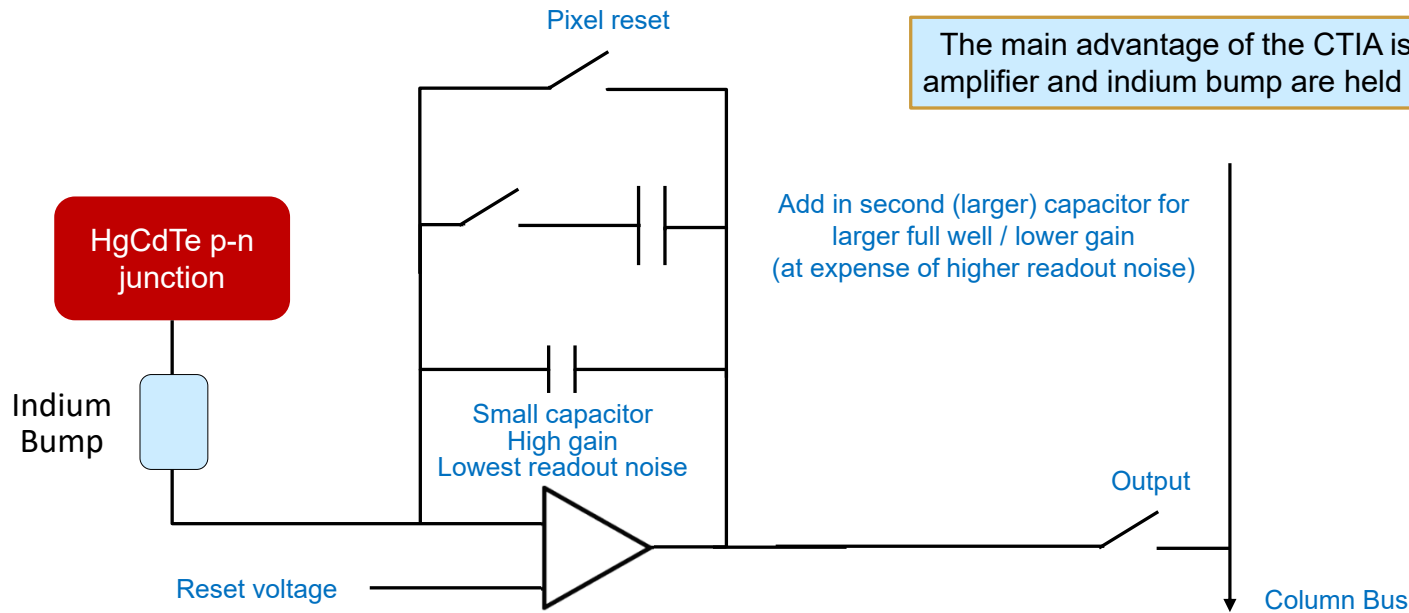


Figures courtesy of Walter Frei, COMSOL Blog, 6 June 2017



Making a higher precision focal plane array (FPA) starts with the Pixel

Better to use a Capacitive TransImpedance Amplifier (CTIA)



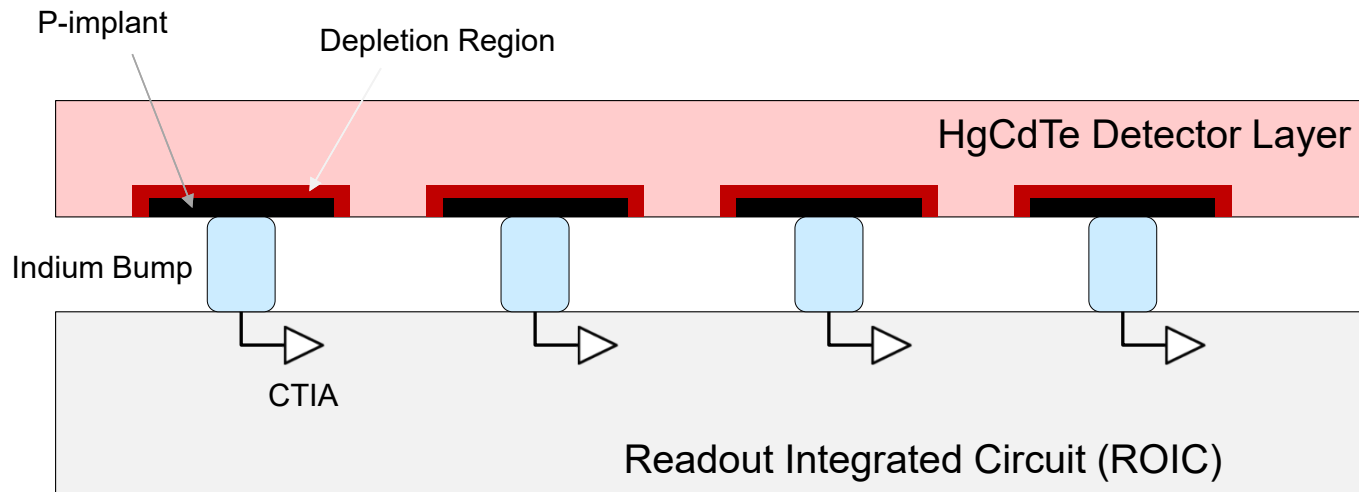
No correlated double sampling (CDS) in this circuit

- For high frame rate operation, such as Earth Observation, CDS is usually included in the pixel.
- Since in-pixel CDS adds circuitry and increases noise, in-pixel CDS not be optimal for an astronomy CTIA array.
- The circuit shown allows “sample up the ramp” for lowest noise and detection of cosmic ray hits.

The challenges for using a CTIA are:

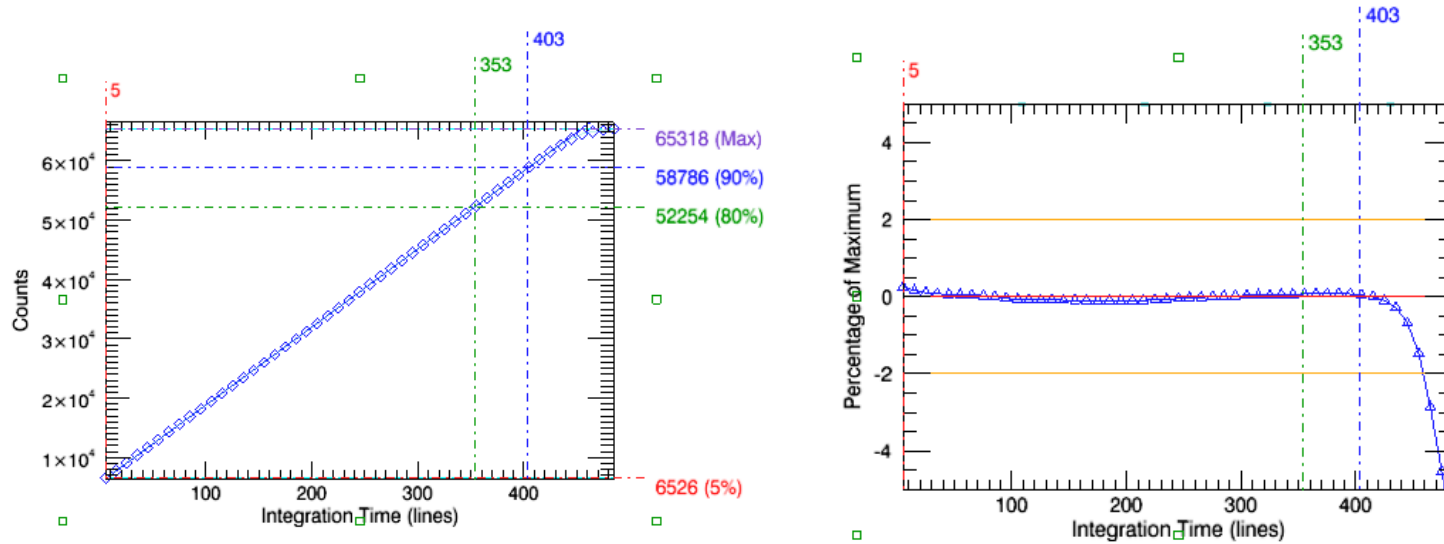
- CTIA must always stay on, so higher power
- Ensuring no ROIC glow
- Achieving low readout noise

CTIA addresses Persistence, IPC, Brighter-fatter effect



- The input gate to all CTIAs are held at the reset voltage during operation (image integration).
- The depletion region stays constant, with no de-biasing and biasing of trap states.
 - This will **eliminate persistence**.
- **No inter-pixel capacitance** since all pixel gates at same voltage.
- **No brighter-fatter effect** since the voltage fields in the HgCdTe stay constant during exposure.

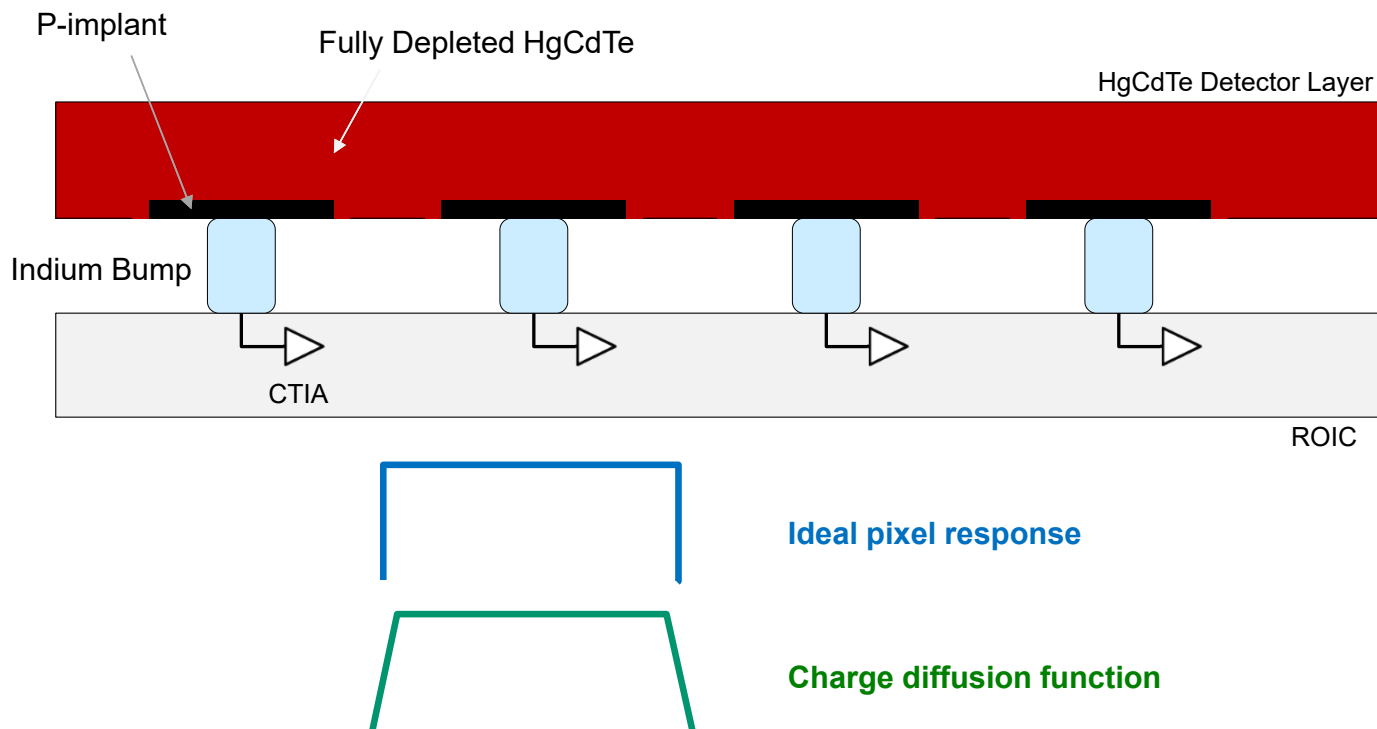
CTIA is highly linear – better than 99.9%



Example from testing of a CHROMA-A CTIA pixel

Optimizing the HgCdTe detector layer

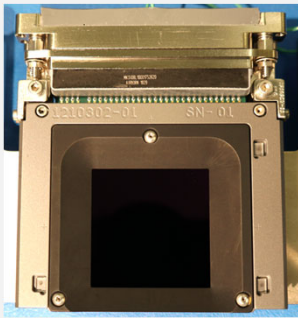
- **Eliminate / minimize cross hatching** with improved growth / processing
- Use low trap passivation process (PV3) developed for RST to reduce persistence (if using HxRG)
- **Minimize charge diffusion** by fully depleting detector layer
 - Charge diffusion function becomes close to an ideal top-hat function



An optimized CTIA + better HgCdTe detector can be a nearly ideal focal plane array

- **Use Capacitive TransImpedance Amplifier (CTIA) pixel**
 - Eliminates:
 - Persistence
 - Inter-pixel capacitance
 - Intensity dependent PSF (no more “fatter-bigger” effect)
 - Produces very linear response
- **Utilize the latest advances in HgCdTe growth and processing**
 - Eliminate cross hatching
 - Use low trap process (PV3) to reduce persistence (if using an HxRG readout circuit)
- **Operate the HgCdTe in fully depleted mode**
 - Sweep charge to p-n junction to minimize charge diffusion
 - Full depletion will also keep traps empty, reducing persistence (for HxRG arrays)

GeoSnap Focal Plane Arrays Use the CTIA Pixel



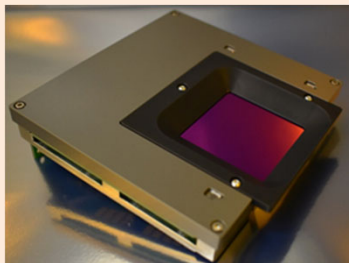
**GeoSnap-18 2K × 2K
Focal Plane Module**

GeoSnap-18

**2K×2K is TRL-9
Operating in Space**

- 18-micron pixel pitch
- **CTIA unit cell** with 2 gains / full well (180 ke- and 2.7 Me-)
- 1K × 512-pixel stitch block, can fabricate up to 3K × 3K pixels
- Snapshot, integrate while read
- Fully digital chip, 14-bit ADCs
- Full frame rate: 100 Hz for 2K × 2K, 250 Hz for 3K × 512
- ROIC formats fabricated: 1K × 512, 2K × 512, 2K × 2K, 3K × 512
- Focal plane arrays made and tested with several types of detectors:
 - Silicon (VNIR) & HgCdTe for SWIR (2.5 μm), MWIR (5.3 μm), VLWIR (14.5 μm)

VLWIR GeoSnap-18
2K×2K FPM
delivered to the
European Southern
Observatory
for the
ELT METIS instrument



**GeoSnap-10 4K × 4K
Focal Plane Module**

GeoSnap-10

**4K×4K is TRL-9
Operating in Space**

- 10-micron pixel pitch
- **CTIA unit cell** with 2 gains / full well (120 ke- and 1.2 Me-)
- 2K × 1K-pixel stitch block
- Snapshot, integrate while read or integrate then read
- Fully digital chip, 14-bit ADCs
- Full frame rate: 60 Hz for 4K × 4K
- Focal plane arrays made and tested with HgCdTe detectors:
 - SWIR (2.5 μm), S/MWIR (3.8 μm), MWIR (5.3 μm)



Teledyne

Enabling humankind to understand the Universe and our place in it



Reserve your calendars!
Scientific Detector Workshop 2025 (SDW2025)
6 – 10 October 2025
Canberra, Australia



A workshop for the scientists and engineers who develop, produce, implement, and operate the most advanced imaging sensors used in scientific instrumentation:

- Talks from leading experts in science, instrumentation, and imaging sensors
- Extensive time for discussions & interactive roundtables
- Group activities include numerous social and cultural events

Hosted by the Australian National University (ANU)



**Activities include tour and dinner
at Mt. Stromlo Observatory**

Sponsors (so far)



For information and sponsorship
email: Tony.Travouillon@anu.edu.au